2 PF Ring

2-1 Summary of Machine Operation

Throughout FY2002, the PF Light Source Division staff maintained the highly reliable operation of the PF ring, improved the performance of the ring, and carried out new developments.

Table 1 gives operation statistics of the PF ring during FY2002. The bar graph in Fig. 1 shows the ring operation time, scheduled user time and effective user time since 1982. The total operation time of the PF ring was 5130 hours. It was slightly shorter than that of FY2001 because the machine operation stopped in March for the upgrade of the PF computer system. Scheduled user time was 4267 hours including 432 hours for single-bunch mode. Effective user time excluding time lost due to machine trouble and daily injections was 4179 hours and its ratio to the scheduled time was 98%. The product of beam current I and beam lifetime τ ($I\tau$) in 2002 was about 1300 A·min (21 A·hour). An improvement of $I\tau$ since the high-brilliance project of 1997 is shown in Fig. 2. We injected the electron beam to the ring at 9 o'clock every day, and the initial beam current of 450 mA was kept at the same value as the previous year. Figure 3 shows a steady increase of the average stored beam current between each injection. Total failure time was 20.8 hours, and the failure rate, defined as the failure time to the total operation time, was about 0.4%. The trend over time of the failure rate is shown in Fig. 4. The failure rate in FY2002 was the lowest during the 21-year operation since 1982. The staff of the light source division and the operators of the PF ring make an effort to foresee various kinds of machine trouble. They try to find small irregularities of the accelerator and peripheral equipment and deal with them before they become major problems. As a result of careful operations, we could attain the lowest ever failure rate.

We have proceeded with an upgrade project of the straight sections of the PF ring as described in the next section. In FY2002, we continued preparatory work for the project. Installation of redesigned front-ends has already been accomplished at seven beamlines. A small number of quadrupole magnets were manufactured and their performance was verified by field measurement. During the summer of 2003, two of them will be installed in the ring for installation of a new multipole wiggler at BL-5. We also proceeded with design work of beam ducts and development of vacuum components such as RF-shield bellows. We are ready to start mass-production of the new quadrupole magnets and vacuum ducts in FY2003.

Table 1 Statistics of the PF Storage Ring Operation during FY2002.

	Multi-bunch	Single-bunch	Total
Ring Operation Time (hours)	4698.0	432.0	5130.0
Scheduled user time (hours)	3835.0	432.0	4267.0
Effective user time T (hours)	3772.8	406.6	4179.4
Time used for injection (hours)	43.3	23.7	67.0
Integrated current in T (A·hours)	1289.9	18.6	1308.5
Average current in T (mA)	341.9	45.7	--
Number of injections	165	55	220
Interval between injections (hours)	22.9	7.4	--

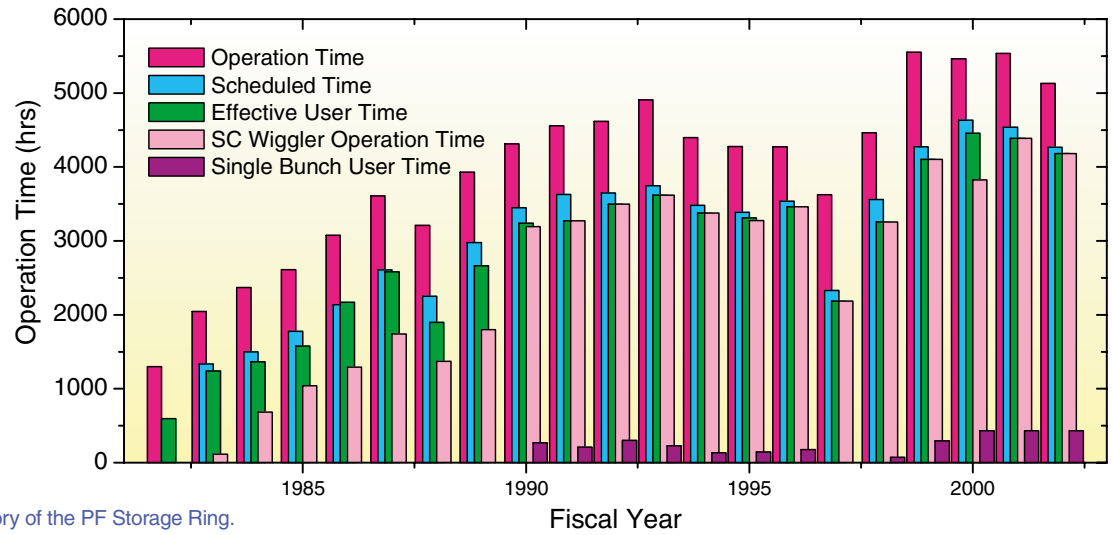

Figure 1
Operation time history of the PF Storage Ring.

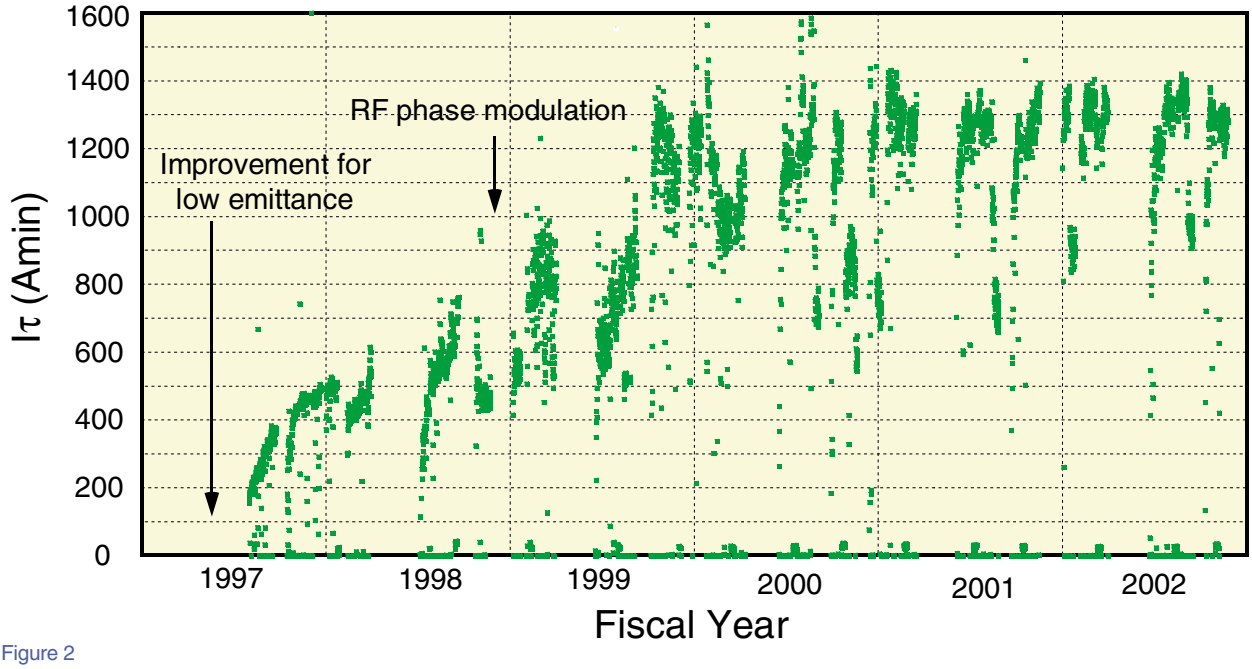

Figure 2
Iτ history of the PF Storage Ring over the past 6 years.

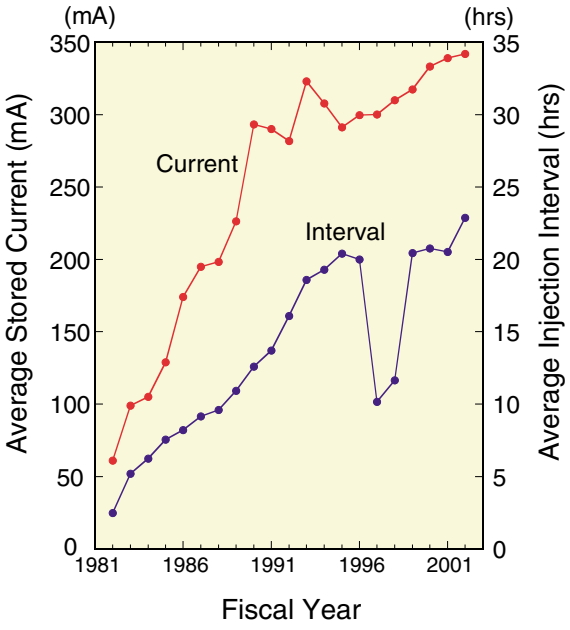

Figure 3
Average current and injection interval of the PF Storage Ring.

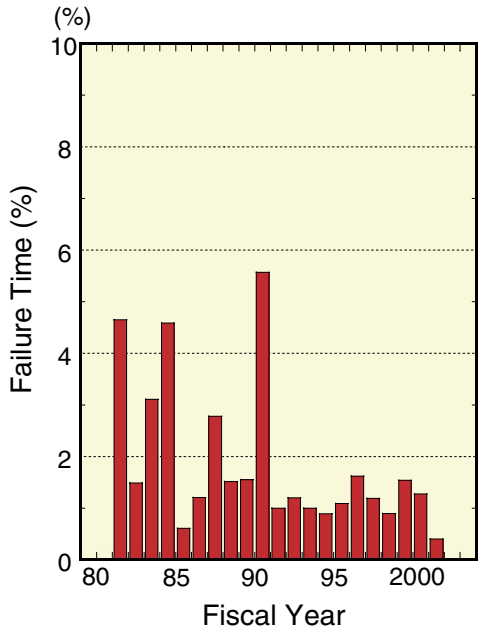

Figure 4
Failure time history of the PF Storage Ring.

2-2 The Straight-Sections Upgrade Project

Overview

In the PF ring, six insertion devices including one super-conducting wiggler are currently installed. The upgrade project [1] is a plan to double the number of straight sections available for insertion devices. As shown in Fig. 5, all quadrupole magnets around the straight sections are to be replaced with new ones having shorter lengths and higher fields in positions closer to their neighboring bending magnets. Short straight sections of 1.4 m will be created by replacing triplet magnets by pairs of doublet magnets as shown in Fig. 6. The lengths of all existing straight sections will be extended. The extension of the longest straight section is shown in Fig. 7. The PF storage ring will then have two straight sections of 9 m length, four of 5.7 m, four of 5 m and four of 1.4 m. When the upgrade alterations are completed, 11 straight sections will be available for insertion devices. In addition, two short insertion devices may be installed in the two 5.7 m-long straight sections where the RF cavities are placed. The dispersion and the betatron functions of these sections will be optimized to be as low as possible. In particular, the vertical betatron function of the short straight section will be reduced to a minimum value of 0.4

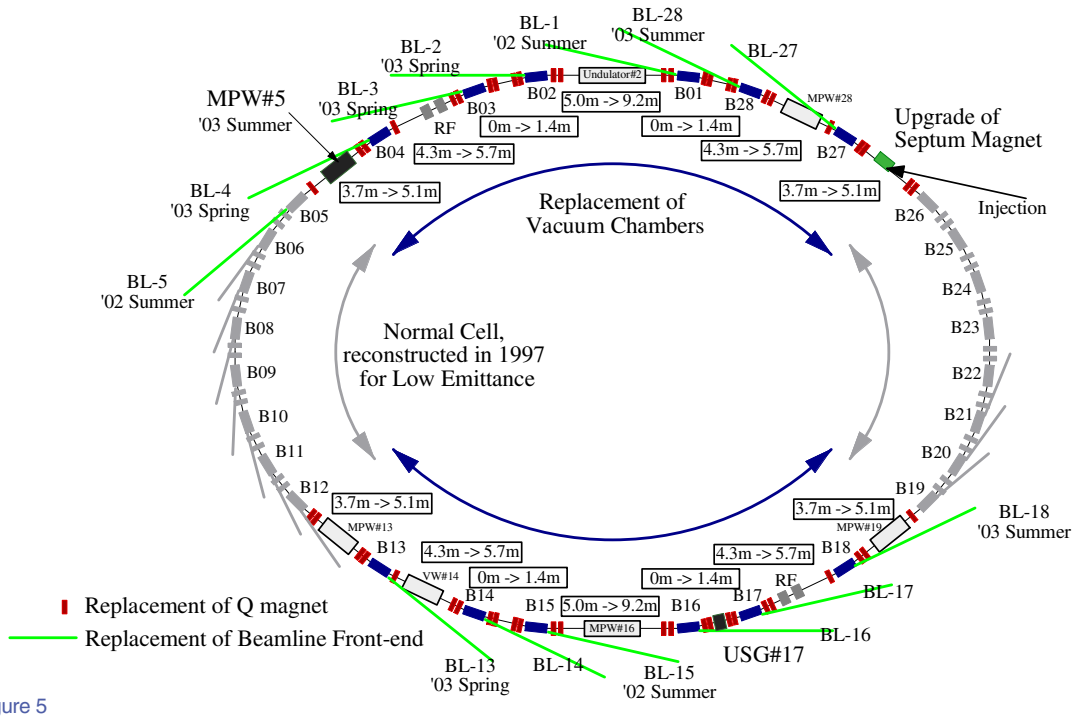

Figure 5
Outline of the upgrade project.

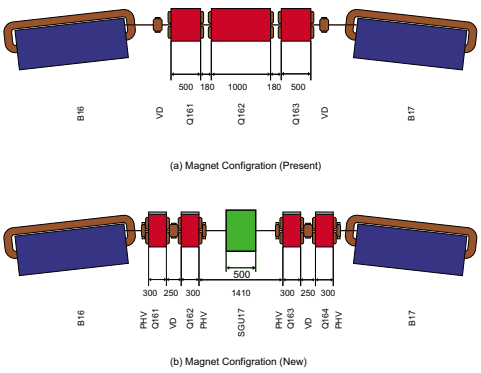

Figure 6
Creation of the short straight section.

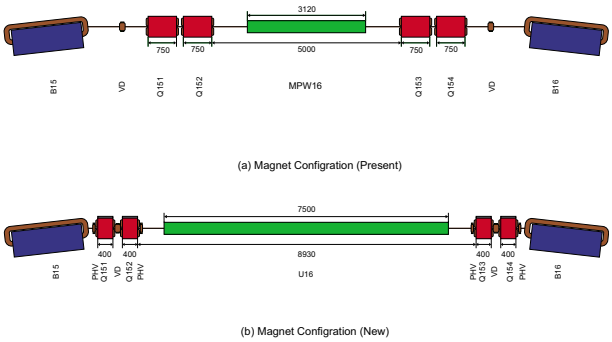

Figure 7
Extension of the longest straight section.

m. A short-period narrow-gap undulator suitable for X-ray research fields is proposed as a light source using the short straight section.

In order to modify the lattice configuration, replacement of the vacuum ducts in two thirds of the storage ring is planned. The replacement of 13 front-ends related to the straight sections will be accomplished prior to the whole reconstruction of the ring. In the autumn of 2003, a new beamline for protein crystallography will be commissioned at BL-5, the last straight section in the present configuration. Installation of a new multipole wiggler into BL-5 is scheduled for the summer shutdown of 2003. At the same time, the two straight sections of B04-B05 and B18-B19 will be partially reconstructed with new quadrupole magnets. It is expected that the whole reconstruction and re-commissioning of the ring will be completed in FY2005.

References

[1] *Photon Factory Activity Report* **2001 #19** (2003) A90.

Design of Beam Chambers

Due to new magnets and the arrangement for the upgrade of the straight sections, a number of vacuum beam chambers including those in twelve bend sections will be replaced with new ones. Some components such as RF cavities, insertion devices and beam diagnostic tools will remain. It is neccessary to maintain the same operation pressure as the present.

The cross-sectional shape of the beam channel has been decided under the following considerations.

1) It should be compatible with the new quadrupole magnet.
2) Its physical aperture must be wide enough to maintain the current vacuum beam lifetime.
3) The sensitivity of the new beam position monitor (BPM) should offer an improvement over the currently used BPM.

As a result, the beam channel becomes slim, and the sensitivity of the BPM is improved twice in the vertical direction without being degraded in the horizontal

direction. The BPM consists of four electrodes with two welded onto the top and two onto the bottom side of the beam chamber through a housing as shown in Fig. 8. The straight chamber with the BPM is installed in the quadrupole magnet and is called the Q-chamber. The total number of BPMs in the ring will be 78 including 44 new ones. The necessary number of BPM housing has already been fabricated. The main material of the beam chamber is unchanged, being aluminum alloy. The necessary amount of aluminum alloy pipes with the required cross section has been extruded to provide the material for the straight chambers.

The conceptual design of each chamber has been carried out. The pumping concept is unchanged. The main pumps used are titanium sublimation pumps, sputter ion pumps and distributed ion pumps. Much effort has been spent on the design of the bend sections. The conceptual design of the bend section is shown in Fig. 9. The B-chamber consists of a bend chamber with a synchrotron radiation (SR) port and a Q-chamber, welded through bellows. The downstream part of the SR port is exchangeable to allow for changes in the SR beamline. A pumping port is located between the bend magnet and the following quadrupole magnet as is the case currently.

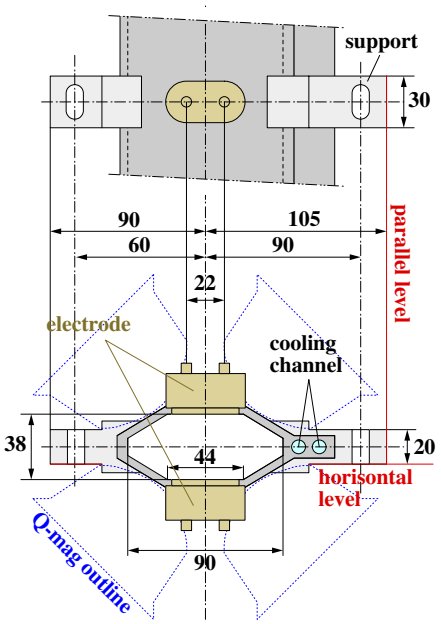

Figure 8
BPM design.

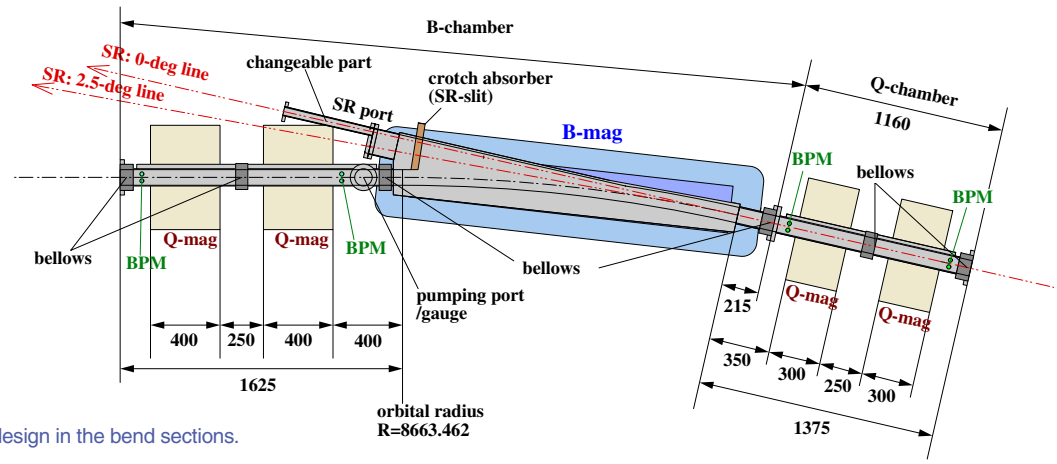

Figure 9
Conceptual chamber design in the bend sections.

This is essential in order to maintain the same operation pressure. The BPM and the crotch part of the SR port are fixed points of installation and there is a bellows with RF contact at their intervals. Two-thirds of the necessary number of bellows have been prepared. Also, for precedent remodeling of the straight sections at B04-B05 and B18-B19, the necessary straight beam chambers including two Q-chambers have already been manufactured. These will be installed in FY2003.

Field Measurement of the New Quadrupole Magnets

During the summer shutdown of 2003, we will replace two quadrupole magnets (Q043 and Q183) to extend the straight sections of B04-B05 and B18-B19. After the lattice rearrangement, these sections will have a longer drift space of about 1.0 m. To achieve the rearrangement, we have designed and produced new quadrupole magnets. The specification of the magnets is given in Table 2. The core length is 200 mm shorter than that of the old magnets. The correction coil is also attached for the correction of tune shifts from the insertion devices.

The field measurement was carried out using a harmonic coil to obtain the excitation curve of the field gradient and the thickness of the end-shims, which reduce the higher order multi-pole components. A photograph taken during the measurement is shown in Fig. 10, and a schematic drawing of the measurement system is shown in Fig. 11.

Table 2 Specifications of the new quadrupole magnets.

Core length	300	mm
Bore radius	35	mm
Maximum field gradient	30	T/m
Maximum current	780	A
Turn number of coil/pole	23	turns
Coil resistance at 75˚	23	mΩ
Maximum voltage	18	V

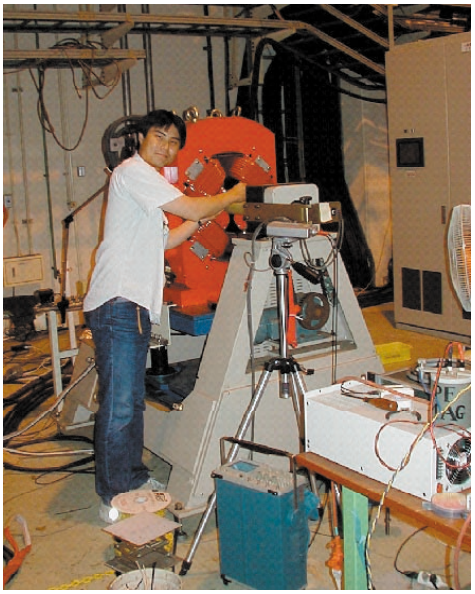

Figure 10
Photograph taken during field measurement.

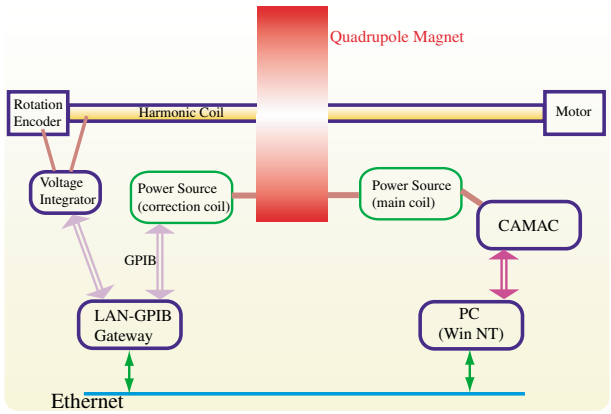

Figure 11
Schematic drawing of the measurement system.

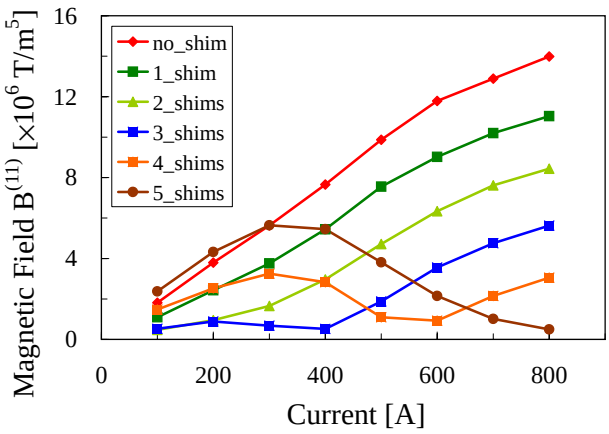

Figure 12
Dodecapole component with several end-shim thicknesses.

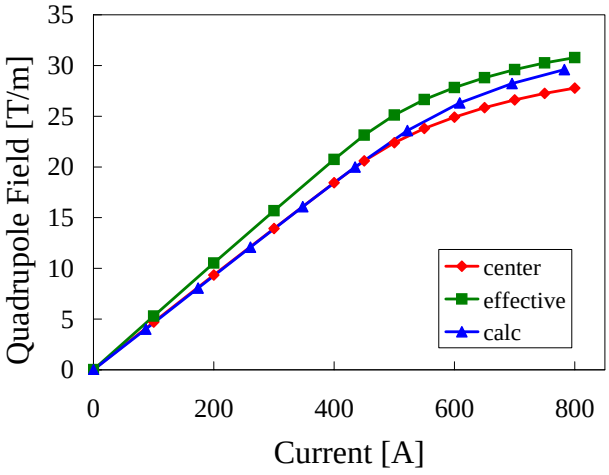

Figure 13
Excitation curves of the field gradient.

The measured results of the dodecapole component with several end-shim thicknesses are shown in Fig. 12. The field gradient of the magnets is required to be from 8.0 to 10.0 T/m in user operation, corresponding to an excitation current of 150 A to 200 A. Thus, we have selected end-shims of 4 mm thickness in order to reduce the dodecapole component as much as possible. The excitation curves of the field gradient are shown in Fig. 13. The red line shows the central field gradient measured by the short coil and the green line the effective field gradient, which is obtained by dividing the integrated field gradient by the core length. The blue line represents the results of a two-dimensional field calculation using POISSON. The measured central field gradient agrees well with the two-dimensional calculation where the field excitation is linear. We observed field saturation when the magnetic current was greater than about 500 A. In this region, the measured central field gradients are smaller than the calculation since the real magnet has a finite length. However, the effective field gradient is larger than that of the 2D calculation, and the gradient at a current of 800 A reaches 30.8 T/m. We are satisfied with the measured results for the field gradients and the strength of the higher order multi-pole components, so we will adopt quadrupole magnets of the same design in the future renewal of other straight sections.

Construction of a New Multipole Wiggler

We are constructing a new multipole wiggler (MPW#05) to be installed in the straight section between bending magnets #04 and #05. MPW#05 will be used exclusively as a light source for the beamline for protein crystallography. For this purpose, the required energy region of the synchrotron radiation is mainly 10 keV to 15 keV. In the design stage, we have tried to optimize the parameters of MPW#05 so that the photon flux density is as high as possible in this energy region, and the magnetic attractive force between the magnet arrays is minimized without a degradation of the field quality. Under the constraints of the proposed accelerator design for the present upgrade, we have found that a combination of a

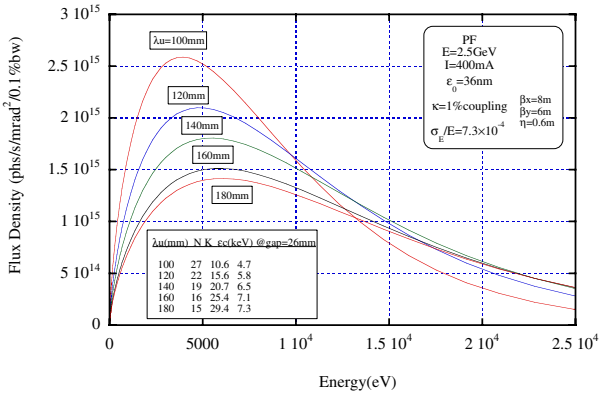

Figure 14
Comparison of the calculated photon flux densities with several period lengths. Total length of the magnet array is kept constant.

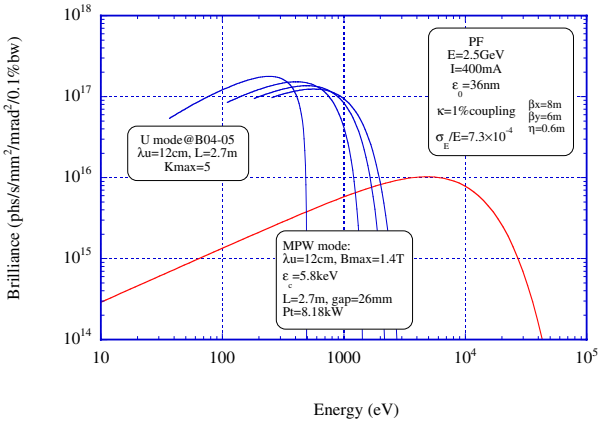

Figure 15
Spectral properties of MPW#05 in the PF ring. In addition to a wiggler mode, the spectra in the case of an undulator mode are shown.

period length of 12 cm and a periodicity of 21 is most suitable for the available length between bending magnets #04 and #05, as shown in Fig. 14.

In order to achieve the required field intensity of 1.4 T at a magnet gap of 26 mm, we adopt a hybrid magnet arrangement: NdFeB is used for the permanent magnet, and vanadium-Permendur for the iron core. The maximum K value is 15.8 at the minimum gap of 26 mm. Calculated spectra of the synchrotron radiation from MPW#05 are shown in Fig. 15: the spectra for the undulator radiation (up to the 7th harmonic) are also shown along with that for the wiggler radiation. The measurement and the adjustment of the magnetic field are performed using a 2-dimentional Hall probe system and a flipping coil system. After the field adjustment, MPW#05 will be installed in the PF ring in summer of 2003, and commissioning started in autumn.

2-3 Low Emittance Operation Study

The natural emittance of the present optics is about 36 nm·rad at 2.5 GeV and the horizontal phase advance of the normal cell about 105 degrees. We have proceeded with a machine study to search for practical operation with an increased phase advance of 125 degrees and a reduced emittance of 28 nm·rad. Figure 16 shows a comparison of the optical functions of the present optics with those of the low-emittance optics in two normal cells. As a result of the stronger focusing power necessary to increase the horizontal phase advance at the normal cell, the chromaticity becomes larger. Thus, stronger sextupole fields are required for chromatic correction, and the resultant large non-linearity reduces the dynamic aperture [1]. In fact, since the dynamic aperture was reduced by about a half compared with the present optics, beam injection became very difficult with the low-emittance optics.

In order to overcome this injection difficulty, we have designed new traveling-wave kicker magnets, which were successfully installed in October 2002. The maximum kick angle of the new kicker magnets is 3.5 mrad. The angles of the kicker and septum magnets for the low emittance optics were optimised by measuring the coherent oscillation of the injected beam by a turn-by-turn position monitor [2], and the obtained injection parameters are listed in Table 3. Since the injection rate shows a strong dependency on the betatron tune, we carried out the tune-survey around the designed tune. A tune point giving an injection rate over 1 mA/s at a repetition rate of 25 Hz was found. Figure 17 shows a typical example of the

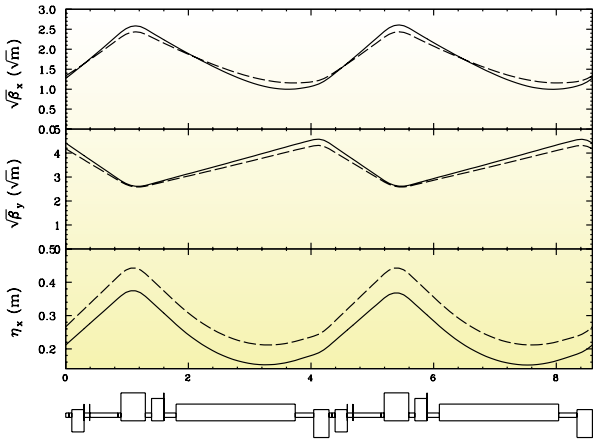

Figure 16
Optical functions of the present and the low emittance optics in two normal cells. The solid line represents the low emittance optics and the dashed line the present optics.

Table 3 Set parameter of the injection magnets. K and S indicate kicker magnets and septum magnets, respectively.

	105 deg	125 deg
K1 (mrad)	2.507	3.107
K2 (mrad)	-1.64	-2.54
K3 (mrad)	2. 28	3.428
K4 (mrad)	2. 12	2.812
S1 (mrad)	117.74	117.64
S2 (mrad)	101.7	102.8

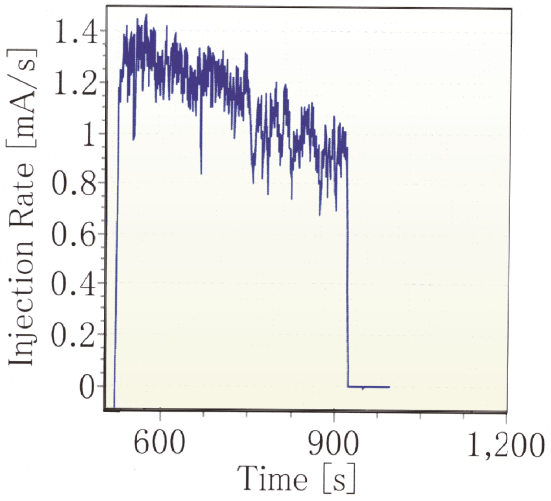

Figure 17
Typical injection history when beam was stored from a current of 0 mA to 450 mA.

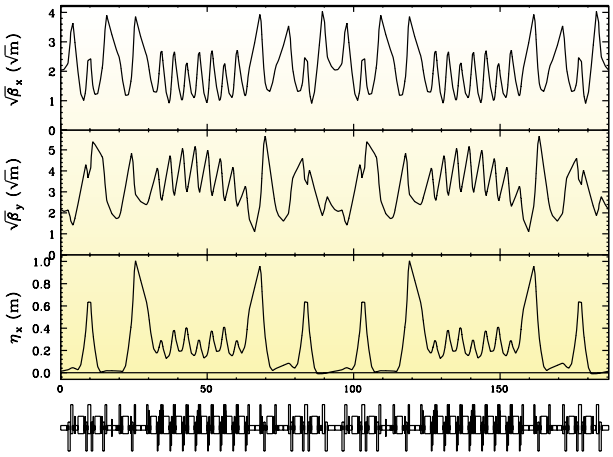

Figure 18
Measured optical functions of the ring with the low emittance optics.

injection rate.

We have also measured the optical functions using the response matrix method, as shown in Fig. 18. The emittance was calculated to be about 28.0 nm·rad. In addition, the betatron tunes were estimated to be (ν_x, ν_y) = (10.42, 4.37). These values agree well with the measured values.

Even with the low emittance optics, the beam lifetime was quite long. With a beam current (I) of 450 mA, the beam lifetime (τ) was over 45 hours giving an $I\tau$ of over 1200 A·min, comparable to the presently used optics. However, this long beam lifetime might be caused by an increase in X-Y coupling. As a next step, we will try to correct the X-Y coupling, and establish practical operation in the low emittance mode in the near future.

References

[1] E. Kim *et al.*, *Jpn. J. Appl. Phys.* **36** (1997) 7415.

[2] Y. Kobayashi *et al.*, *Proc. of EPAC,* Spain (1996) 1666.

2-4 Beam Instability Studies Using a Pulsed Octupole Magnet

In the PF Storage Ring, a vertical instability is observed in multi-bunch operation mode, which is suppressed by a DC octupole magnetic field in routine operation. It seems that the instability is caused by ion trapping effect, the operating parameters in routine operation are near the threshold for this to occur, and the Landau damping caused by the octupole field suppresses the instability [1]. In order to study the dynamical behavior of the instability, we have developed a pulsed octupole magnet system which can produce an octupole field with rise and fall times of around 1.2 ms [2]. Since we installed the magnet system in the PF-ring at the end of 2001, intensive machine studies have been carried out.

The principal parameters of the pulsed octupole magnet system are given in Table 4. It consists of a magnet, a ceramic duct and a power supply. The pulsed octupole magnet was designed using a computer code POISSON to realize a maximum field gradient of 11700 T/m^3 at an excitation current of 1000 A·turns and a self-inductance of about 3 mH. In order to realize a high field gradient, the bore diameter of the magnet was designed to be 80mm. To reduce the inductance, the turn number of the coil is 10 turns per pole giving a calculated inductance of 3.24 mH, and the measured inductance was 3.34 mH. A cross-sectional view and a photograph of the pulsed octupole magnet are shown in Figs. 19 and 20. The iron

Table 4 Principal parameters of the pulsed octupole magnet system.

Parameter	value
Maximum field gradient (pea)	11700 T/m^3
Maximum pea current	100 A
Maximum pea voltage	285
Bore diameter	80 mm
Core length	0.20 m
Effective length	0.22 m
Self inductance	3.34 mH

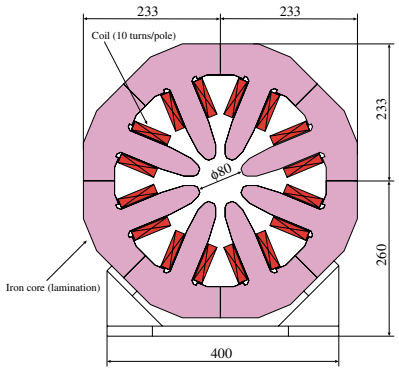

Figure 19
Cross sectional view of the pulsed octupole magnet.

Figure 20
Photograph of the pulsed octupole magnet installed in the PF ring.

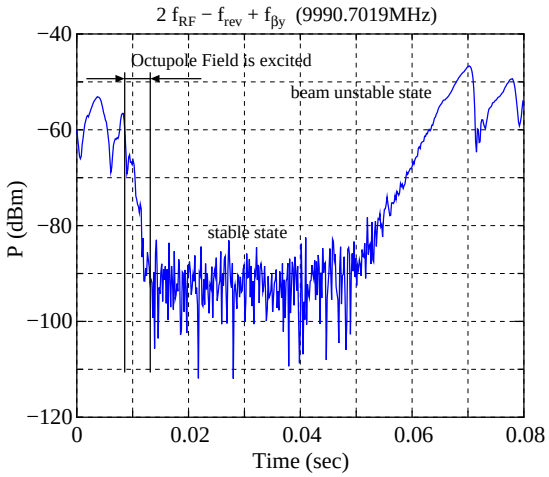

Figure 22
Power of the vertical instability at $2f_{RF} - f_{rev} + f_{\beta y}$. The pulsed octupole magnet was excited at 100 A from t = 8 ms to 12.8 ms.

core is made from 0.5-mm thick silicon steel lamination and the length is 0.2 m.

In order to investigate the behavior of the beam instability when the pulse octupole field was applied, we measured the frequency spectrum of a button-electrode signal using a real-time spectrum analyzer. The ring parameters were set in the vicinity of the threshold of the instability suppression. Under these conditions, the instability was suppressed only when the pulse octupole magnet was excited. Figure 21 shows the beam spectrum observed as sidebands of the second harmonic of the RF frequency (f_{RF}) when the pulsed octupole magnet was excited at 100 A. Here, the beam current was 400 mA filled in 280 bunches. Figure 22 shows the power of the vertical instability at $2f_{RF} - f_{rev} + f_{\beta y}$, where f_{rev} and $f_{\beta y}$ are the revolution and vertical betatron frequencies. Immediately after excitation of the magnet, the power spectra of the instability decreased, i.e., the instability was suppressed. About 50 ms later, the instability grew slowly in contrast with the quick response of suppression. It seems that the difference between the growth time and the suppression time is caused by difference in the mechanisms between ion trapping and Landau damping. In order to investigate the effect of ion trapping, we plan to study the dependence of the instability on beam current and on the fill pattern of the bunch train.

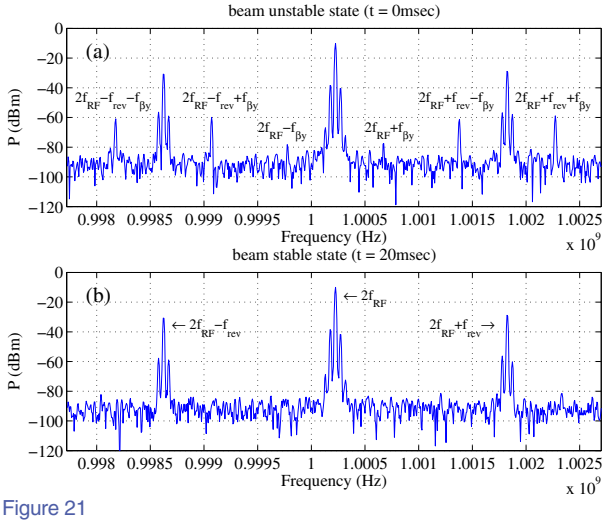

Figure 21
Beam spectrum from a button electrode. a) The spectrum when the vertical instability was excited at t = 0 ms (b) The spectrum when the instability was suppressed at t = 20 ms.

References

[1] Y. Kobayashi *et al.*, *Proc. of EPAC98*, Stockholm 1998.

[2] T. Miyajima *et al.*, *Proc. of the 2003 Particle Accelerator Conference,* Portland, 2003 (to be published).

2-5 Measurement of Transverse Quadrupole-Mode Frequencies of an Electron Bunch

According to the theories of collective beam dynamics [1], the motion of a bunched beam can be described by a superposition of many normal-modes of oscillation. The lowest mode (dipole mode) of such oscillations represents a center-of-bunch oscillation, while higher modes (quadrupole-mode, sextupole-mode, etc.) represent various oscillations in the bunch-shape.

In many electron storage rings, it has been observed that the frequencies of the transverse dipole oscillations

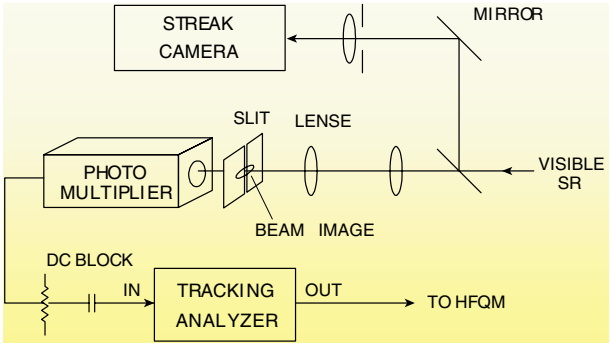

Figure 23
Experimental setup for measuring the transverse quadrupole frequencies.

depend on the bunch current (i.e. the beam current per bunch) [2,3] due to transverse wake forces. However, there have been few measurements on the frequencies of higher-mode oscillations. We expect that such investigations will enrich our knowledge of collective beam behavior.

Due to this motivation, we have measured [4] the frequencies of the transverse coherent quadrupole oscillations in the PF storage ring. The experimental setup is depicted in Fig. 23. While storing a single bunch of electrons, we induced transverse quadrupole oscillations by applying a small tune modulation ($\delta\nu_x = 5.2 \times 10^{-5}$) at a frequency of about twice the fractional betatron frequency ($2f_{\beta x}$ 1.915 MHz) [5]. Excited quadrupole oscillations were detected as an intensity modulation of the synchrotron light from the central part of the bunch, using a photo multiplier. The responses of such oscillations on the excitation frequency were measured under different bunch currents.

Some of the measured beam responses are shown in Fig. 24. Each trace in Fig. 24 shows a peak, indicating a coherent, horizontal quadrupole frequency. Figure 25 shows a summary of the measured quadrupole frequencies. We have found that the horizontal quadrupole frequency shifted higher as the bunch current increased; the dependence on the current was about 0.077 kHz/mA.

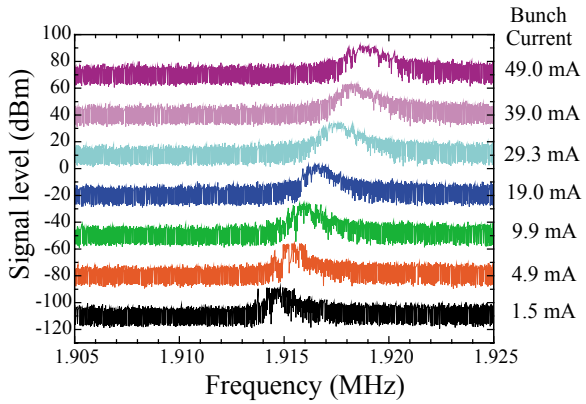

Figure 24
Responses of the horizontal quadrupole oscillation on the excitation frequency. The measurement was carried out under different bunch currents.

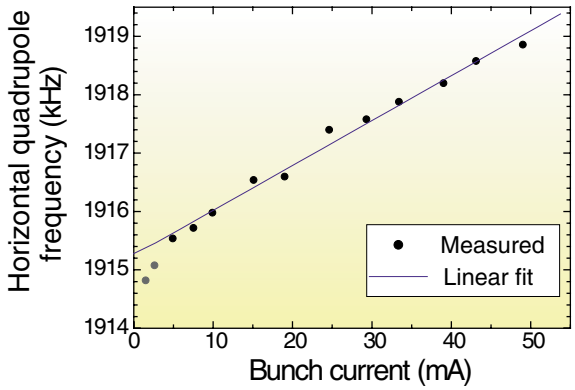

Figure 25
Measured coherent frequencies of the horizontal quadrupole oscillation.

This result contrasts well with the measured dipole frequencies; the horizontal dipole frequency shifts down with the bunch current by about –0.029 kHz/mA. It is worth noting that the quadrupole frequency (about 1.915 MHz) at low currents was very close to twice the fractional horizontal betatron frequency ($f_{\beta x}$) of about 957.5 kHz.

The above result reveals an interesting aspect of collective beam phenomena which is possibly due to transverse wake forces.

References

[1] A.W. Chao, *Physics of Collective Beam Instabilities in High Energy Accelerators*, John Wiley & Sons, New York, 1993.
[2] J.C. Denard *et al.*, *IEEE Trans. on Nucl. Sci.* **NS-28** (1981) 2474.
[3] D. Rice *et al.*, *IEEE Trans. on Nucl. Sci.* **NS-28** (1981) 2446.
[4] S. Sakanaka, T. Mitsuhashi and T. Obina, to be published in *Proceedings of the 2003 Particle Accelerator Conference (PAC2003)*, Portland, U.S.A, May 12-16, 2003.
[5] S. Sakanaka, Y. Kobayashi, T. Mitsuhashi and T. Obina, *Jpn. J. Appl. Phys.* **42** (2003) 1757.

2-6 Polarization Control by a New Arrangement of Undulator Magnets

The capability to rapidly switch circular polarization via linear polarization is now becoming a requirement for new circularly polarized undulator sources. Most recent attempts to meet this requirement adopt either (1) electrical switching of electromagnets, or (2) a tandem configuration of left-handed and right handed undulators, as seen in several third generation synchrotron radiation facilities.

At the 2.5-GeV PF ring, we find that electro-magnets are not the most suitable for the production of soft X-ray or higher energy photons, and we also desire to utilize the full length of a straight section instead of splitting it into two halves. As a result of studies along these lines, we have come up with a completely new scheme which employs permanent magnets and mechanical switching.

Our new undulator consists of upper and lower magnet arrays, as usual. However, the magnets in each array are arranged with an oblique angle to the axis of the array just like a half of a chevron mark. The upper array has the opposite sign of this oblique angle (hereafter we call a chevron angle) to the lower array. When this chevron angle is equal to zero, the arrangement is identical to the pure Halbach type. We have devised a new mechanism by which we can control the polarization of the radiation from left-handed circular to right-handed circular via linear by changing the chevron angle. A test-stand employing this magnet arrangement with 5 periods × 6-cm period length has been built recently. A result of the magnetic measurements made for this test-stand are summarized in Figs. 26(a) and 26(b). A switching rate of about 1 Hz has been achieved so far.

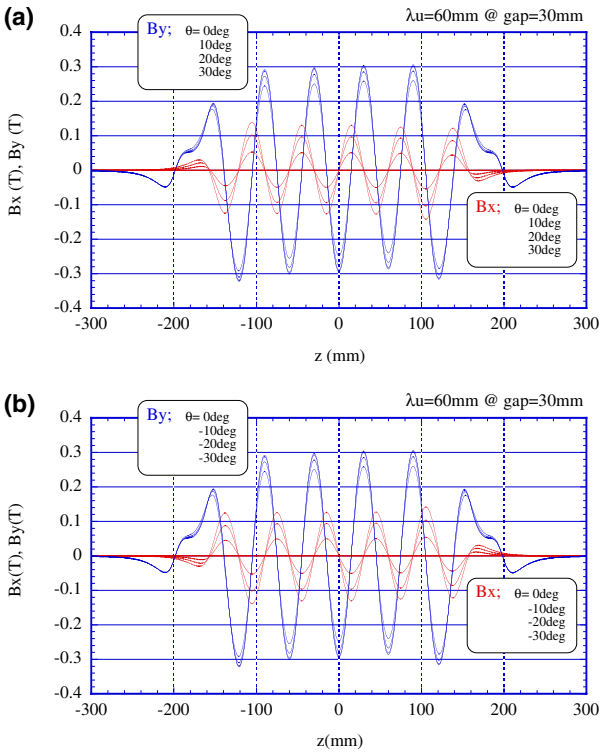

Figure 26
The horizontal (Bx) and vertical (By) magnetic field are shown for several chevron angles (a). Cases for the opposite chevron angles are shown (b): It is noted that the phase of the horizontal field is shifted by a half period of the magnetic field.

2-7 Upgrade of the Photon Factory Computer System

The Photon Factory computer system consists of two subsystems, that is, servers for general purpose and a server for accelerator control. The former are used for data processing from experiments, calculations for theoretical physics, accelerator engineering and so on. The latter processes control tasks and a database and acts as the main server of the control system for the storage ring.

The whole system was upgraded in March 2003. The main servers for general purpose were replaced with nine PRIMEPOWER400's from Fujitsu. A log-in server and a file server were also introduced. The total computing power is now about 24,000 SPECfp2000, which is 6 times greater than that of the previous system. The general purpose server system also includes 5.5 TB of RAID storage and a tape library of maximum capacity 28 TB.

The server for the storage ring control was upgraded to an rp5470 from Hewlett-Packard which has a computing power of about 2,000 SPECfp2000, 2.6 times greater than that of the previous server. The attached RAID storage has about 1-TB capacity. The control system also includes many PC's and VME's for local controls and operator consoles.

Firewall systems were placed between the public network and the private networks for security.

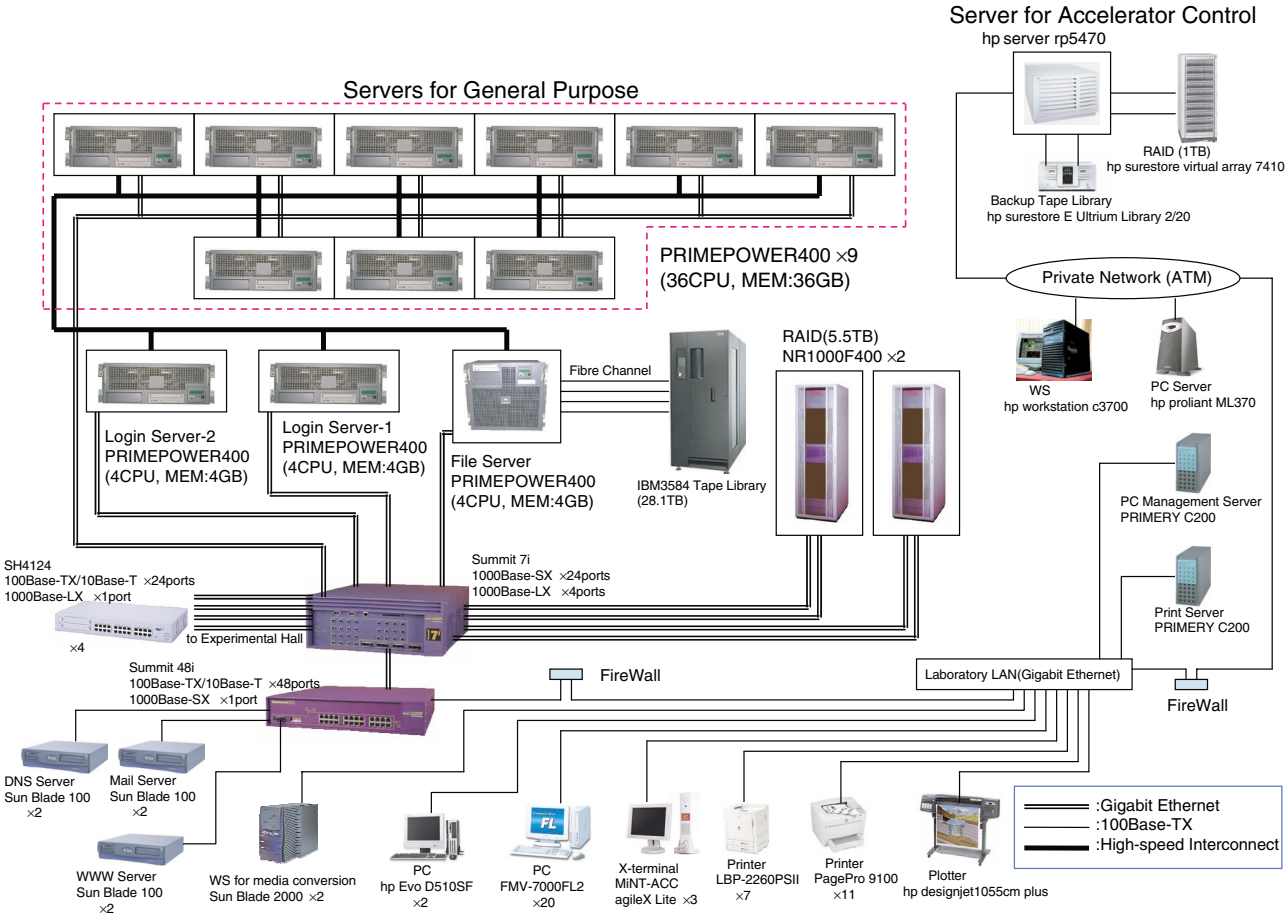

Figure 27
Block diagram of the upgraded computer system.